NASA Technical Memorandum

NASA TM - 82568

THE NEW MSFC SOLAR VECTOR MAGNETOGRAPH

Center Director's Discretionary Fund

Final Report

By M. J. Hagyard, E. A. West, N. P. Cumings
Space Science Laboratory

February 1984

National Aeronautics and Space Administration

George C. Marshall Space Flight Center

MSFC - Form 3190 (Rev. May 1983)

TECHNICAL REPORT STANDARD TITLE PAGE

1. REPORT NO.	2. GOVERNMENT ACCESSION NO.	3. RECIPIENT'S CATALOG NO.
NASA TM-82568		

4. TITLE AND SUBTITLE
The New MSFC Solar Vector Magnetograph
Center Director's Discretionary Fund, Final Report

5. REPORT DATE
February 1984

6. PERFORMING ORGANIZATION CODE

7. AUTHOR(S)
M. J. Hagyard, E. A. West, N. P. Cumings

8. PERFORMING ORGANIZATION REPORT #

9. PERFORMING ORGANIZATION NAME AND ADDRESS
George C. Marshall Space Flight Center
Marshall Space Flight Center, Alabama 35812

10. WORK UNIT NO.

11. CONTRACT OR GRANT NO.

12. SPONSORING AGENCY NAME AND ADDRESS
National Aeronautics and Space Administration
Washington, D.C., 20546

13. TYPE OF REPORT & PERIOD COVERED
Technical Memorandum

14. SPONSORING AGENCY CODE

15. SUPPLEMENTARY NOTES
Prepared by Space Science Laboratory, Science and Engineering Directorate

16. ABSTRACT

The unique MSFC solar vector magnetograph allows measurements of all three components of the Sun's photospheric magnetic field over a wide field-of-view (≈ 6x6 arc min) with spatial resolution determined by a 2.7x 2.7 arc second pixel size. Supported by two Center Director's Discretionary Fund Projects, this system has recently undergone extensive modifications to improve its sensitivity and temporal response. The modifications included: replacing an SEC vidicon detector with a solid-state CCD camera; replacing the original digital logic circuitry with an electronic controller and a computer to provide complete, programmable control over the entire operation of the magnetograph; and installing a new polarimeter which consists of a single electro-optical modulator coupled with interchangeable waveplates mounted on a rotating assembly. In this report, we describe the new system, and present results of calibrations and tests that have been performed. Initial observations of solar magnetic fields with the new magnetograph are presented; they indicate that the system is an order of magnitude more sensitive than the original one and has a much higher temporal response (by a factor of ≈30). These new capabilities enhance our continued research in solar vector magnetic fields and our support of NASA's solar missions.

17. KEY WORDS	18. DISTRIBUTION STATEMENT
Solar magnetograph Polarization measurement Solar instrumentation	Unclassified-Unlimited

19. SECURITY CLASSIF. (of this report)	20. SECURITY CLASSIF. (of this page)	21. NO. OF PAGES	22. PRICE
Unclassified	Unclassified	29	NTIS

MSFC - Form 3292 (May 1969)

For sale by National Technical Information Service, Springfield, Virginia 22151

FINAL REPORT

MSFC CENTER DIRECTOR'S DISCRETIONARY FUND

(Project Numbers 81-12 and 82-8)

The New MSFC Solar Vector Magnetograph

M. J. Hagyard (PI, 81-12)
E. A. West (PI, 82-8)
N. P. Cumings (Project Manager)

Summary Objective: The objective of these programs was to develop new and innovative techniques in polarimetry and signal detection utilizing state-of-the-art technology. This objective arose from the need to observe the Sun's vector magnetic fields with enhanced sensitivity and temporal response, thereby allowing weaker fields outside active regions and rapid evolution everywhere to be measured. These capabilities enhance our continued research in solar vector magnetic fields and our support of NASA's solar missions.

1. Introduction

The ability to adequately characterize the Sun's vector magnetic field is essential to understand the various solar phenomena which intrigue the solar astronomer and which directly or indirectly affect our terrestrial environment. The vector magnetic field is an integral part of magneto-hydrodynamic models of coronal transients, prominences, coronal holes, and sunspots. The magnetic field is invoked as a fundamental aspect of prevalent solar flare theories, for pre-flare energy build-up, as the energy storage medium, and as it allows and affects the eruptive, often impulsive, release of this energy in flares. A great deal of what we know about solar magnetism, its sub-photospheric origins, its role in the solar cycle, and thus its influence on solar-terrestrial relations, comes from observations of the magnetic field with solar magnetographs. The MSFC magnetograph has been unique among such instruments since it is a "vector" system, measuring all three components of the magnetic vector; now there are three such systems operating occasionally around the world, but the MSFC instrument observes most frequently and is the only operational vector magnetograph in the continental United States. This small number of vector magnetographs is a direct consequence of the difficulties encountered in designing a system to measure all three components of the magnetic vector. With the MSFC system we successfully overcame these difficulties through the application of novel polarimetric techniques and detector technology, thereby achieving sensitive detection of weak polarization signals and allowing the derivation of the magnetic vector from a polarimetric analysis of solar radiation. This analysis is based on the Zeeman effect which causes a spectral line

formed in the presence of a magnetic field to be split into several components, each with a characteristic state of linear or circular polarization. Thus, the aggregate spectral line emitted by a solar plasma permeated by a uniform magnetic field has spectral distributions of intensity with well-defined polarization properties; through careful analysis of these polarized intensities, the orientation and strength of the magnetic field can be obtained.

The MSFC vector magnetograph system began as a joint effort between the Naval Research Laboratory and MSFC with the objective of building and operating a ground-based instrument at MSFC to measure vector magnetic fields in active regions on the Sun. Measurements of vector magnetic fields have been made with this system since 1976. During the period of operations of the Solar Maximum Mission (SMM) satellite (February-November 1980), the magnetograph was operated on a daily basis to acquire magnetic field data for later collaborative investigations with SMM experimenters, in particular, those associated with the Ultraviolet Spectrometer and Polarimeter experiment onboard the satellite. As a result of this collaborative data-collection effort, vector magnetic field measurements were available for the analysis of SMM data and have been widely used in SMM-related publications. Upon termination of SMM observations in late 1980, two Discretionary Fund projects were initiated to modify the original magnetograph with the goal of improving its sensitivity and temporal response.

The need for these improvements came from the realization that, although a great deal of unique research resulted from the observational data acquired with the original system (see attached bibliography), the system's limited sensitivity and slow cycle time prevented our investigation of solar phenomena associated with magnetic fields either too weak or evolving too rapidly to be detected. By increasing the system's sensitivity, measurements of the weaker fields outside sunspots in active regions could be made, providing important information on the vector nature of emerging fields as active regions develop, and on the process of flux removal when sunspots decay and disappear. Increased sensitivity might also permit detection of transverse magnetic fields in the supergranular network outside active regions; this would provide solar physicists further insight into this network structure and its implications for models of the solar dynamo. Shorter time response coupled with increased sensitivity is necessary if we are to detect in the vector magnetic field the photospheric signatures of transient changes in electric currents flowing in the solar chromosphere and transition region. These transitory currents have been proposed as the heating source for the transient brightenings seen in uv observations from SMM. Increased temporal response and sensitivity are also essential for investigations of rapid and/or subtle magnetic field changes in solar flares, whether transient or permanent in nature. Observations of transient ($\lesssim$100s) changes indicate they occur mainly in the transverse field component and are thus undetected by conventional, line-of-sight magnetograph observations when the flares erupt in active regions near the center of the solar disk[1].

From these and similar considerations, it became clear that a significant enhancement of our research program would accrue from an upgrading of the original magnetograph. That system, described in [2],

consisted of the telescope, polarizing optics, filter and vidicon detector shown in Fig. 1. The telescope, an f/13, 30 cm-diameter Cassegrainian system, focuses a 3.5 cm image of the Sun on a mirrored aperture stop which limits the field-of-view of the transmitted image to 5.7x5.7 arc minutes; the unused portion of the image is reflected out of the optical path of the magnetograph, to be intercepted by the optics of the correlation tracker (not shown in Fig. 1) which is used for image stabilization. The original polarizing optics consisted of two KD*P (potassium dideuterium phosphate) crystals, and a MgF (magnesium fluoride) crystal which was used to extend the acceptance angle of the two KD*P crystals. The Zeiss birefringent filter has a 0.122 Å bandwidth centered on the FeI 5250.22 Å spectral line; the filter can be tuned $\pm$ 8.0 Å in steps of 0.010 Å. The detector for the original system was a SEC (secondary electron conduction) vidicon tube (Westinghouse WL 31439) with a fiber optics faceplate; the magnetically-deflected read beam scanned the SEC target in 128 discrete horizontal steps along 128 discrete lines.

SEC vidicons were state-of-the-art systems when the MSFC magnetograph was designed over a decade ago, but their sensitivity is limited in comparison with today's solid state detector devices. To take advantage of advances in detector technology, one modification undertaken to upgrade the performance of the MSFC magnetograph was replacement of the SEC vidicon with a CCD (charge-coupled device) camera. At the same time, it was recognized that the benefit of an improved detector would be compromised unless improvements were made in the polarimeter of the magnetograph to increase its sensitivity to a level comparable to the enhanced sensitivity of the new detector. To this end, the upgrading program for the MSFC magnetograph combined the design and installation of both a CCD camera and a new polarimeter to achieve sufficient sensitivity to detect weaker vector fields outside of sunspots and to obtain useful vector magnetograms at a rapid cadence.

2. The New Polarimeter

The primary limitation on the sensitivity of the original polarimeter was the occurrence of field-of-view errors [3] introduced by the two KD*P crystals which were used as variable-retardance waveplates. These errors are a consequence of the inherent birefringence of a KD*P crystal, and they result in undesirable variations over the field-of-view in the retardation induced by the KD*P. For a polarimeter using two KD*P crystals in sequence, the problem is exacerbated, with resulting errors in retardation of up to 25% over a 5.7 arc min field-of-view. In the new polarimeter, one of the two KD*P's in the polarizing optics is replaced by a rotating wheel assembly which allows three non-birefringent waveplates mounted on the wheel to be inserted sequentially into the beam; this assembly is depicted in the schematic drawing shown in Fig. 2. Accurate positioning of the waveplates in the optical path of the magnetograph is controlled electronically: a light-emitting diode (LED) and detector are positioned on either side of the wheel which has small holes precisely located so that a waveplate is in position when the LED source is detected through the corresponding aperture. The three plates are: a single glass window and two quarter-waveplates with their fast axes oriented $\pm 22\frac{1}{2}^{\circ}$ with respect to the analyzer. The other part of the new polarimeter, consisting of a single KD*P and a MgF correction plate, is mounted in a unique clam-shell holder that was specially designed

at MSFC for this purpose. This assembly is located directly behind the rotating waveplate wheel as shown in Fig. 2. Successive rotation of the three waveplates into the solar beam and electro-optical modulation of this KD*P allow the polarization analysis originally performed with two modulated KD*P crystals to be duplicated exactly by this system. The MgF correction plate is used to reduce the field-of-view errors introduced by the birefringence of the remaining KD*P crystal. This unique correction plate is the result of research performed at MSFC by E. A. West [3], and its use significantly decreases field-of-view errors.

The new polarimeter can be seen in the photograph, Fig. 3, which shows the optics box of the new magnetograph. The polarimeter is located just to the right of center of the box; it consists of the wheel assembly and KD*P modulator, as indicated on the figure, and the polarimeter motor and electronics in the lower right corner. The solar beam from the telescope enters the optical train of the magnetograph through the opening in the optics box at its right end.

Tests conducted with the new polarimeter indicate that it is significantly more sensitive than the one previously used. As noted above, the primary limitations on sensitivity are the field-of-view errors introduced by the KD*P that result in variations in retardation over the field-of-view. In tests to determine the level of these variations, known states of linear polarization were introduced into the optical light path and the resulting intensities were recorded and analyzed. In these tests, areas from the center and the left corner of the field-of-view were used to calculate measured percent polarizations. Since there should be no variation in percent polarization over the field in an ideal polarimeter, differences in polarization between these two areas were interpreted as variations in retardation. The results of the tests are shown in Table I. Even the worst case of a 4^{o} error in retardation is well below the theoretical prediction of 10^{o} for a similar optical configuration of a single KD*P. This result is taken to prove the effectiveness of this polarimetric design.

3. The CCD Camera System

Preliminary studies assessing recent advancements in detector technology indicated that a CCD device possessed the required signal-to-noise ratio (S/N), dynamic range, sensitivity, and uniformity to make it suited for application as the detector for the magnetograph. However, a typical CCD camera operates in a continuous-scan mode at a fixed frequency. This meant that modifications would have to be made to operate such a camera in the unconventional mode required by the magnetograph system, where the camera exposures must be synchronized with the electrical switching of the KD*P. The necessary modification required interruption of the exposure of the CCD array during the time interval when the KD*P is switched; this has been accomplished by using an electro-optical shutter synchronized with the CCD camera control system.

The CCD sensor and associated camera and control system were purchased as a unit from Photometrics, Ltd., who designed and manufactured the camera. The sensor chip is an RCA SID 53612, which is a thinned, glass-laminated, all-buried channel CCD with 320x512 pixel elements; the CCD is fabricated

for backside illumination. Of the 320x512 pixels, an array of 256x256 is used for the actual imaging section, while the remaining section is used for temporary storage of data from the imaging array. The pixel transfer rate from the imaging to storage section is 256 kHz, or 4μ sec, for each line of 256 pixels. For the 256 lines of the image array, this results in a total transfer time of 0.001s.

The control system for the CCD camera is quite versatile, incorporating several features designed specifically for the MSFC magnetograph. One of these features is a "binning" capability whereby the signals of adjacent pixels can be binned or combined to form a "super-pixel," resulting in a S/N of the super-pixel which is enhanced with respect to the S/N of a single pixel. In the usual mode of operation of the magnetograph, a 2x2 binning process is used which results in a 128x128 data array with 2.7 arc second pixel size. The camera employs correlated double-sampling of pixels to eliminate gate noise. The read-out rate from the storage array is 6.3μ s per "binned" pixel; this results in a total read-out time of 0.1s for the 128x128 array. The quoted quantum efficiency for the RCA chip is 80% at the wavelength at which the magnetograph is operated (5250 Å). To decrease noise, the CCD chip is cooled by a thermo-electric cooler which keeps the operational temperature of the CCD at $\approx$ 40 C below ambient temperature. In Fig. 3 the CCD camera and the electro-optical (KD*P) shutter assembly can be seen in the left portion of the photograph.

Data from the 12-bit analog-to-digital (A/D) converter of the CCD camera system go directly into a high-speed adder and microprocessor system containing two 128x128x22-bit memories for the storage of sums of 128x128x12 bit CCD data. Using these two memories, two polarized image arrays can be temporarily stored and "enhanced" by the successive adding of similarly-polarized images; this enhancement process results in an increased signal-to-noise ratio for the data. The microprocessor controls all operations of the CCD camera, shutter, and other components of the magnetograph. The microprocessor is itself controlled via a programmable minicomputer data system consisting of a PDP 11-23 computer with a 512 kilobyte memory, control terminals, color-graphics display monitor, line printer, two (150 and 300 megabyte) disk systems, and tape recorder. This data system's software provides all of the necessary commands to operate the magnetograph and acquire data, as well as to display analog or processed images, store information on disk, perform data analyses with graphics display and hardcopy output, and transfer data to magnetic tape for permanent storage.

4. The Integrated System

The newly-upgraded MSFC vector magnetograph, with refurbished telescope mirrors and optics box, was reinstalled at the observing site in May 1983. The complete integrated system is shown in the schematic drawing of Fig. 4. In Fig. 5, the layout of the optics box is shown in more detail, indicating the components developed in these Discretionary Fund programs; the actual hardware can be seen in Fig. 3. The complex interfaces among the magnetograph components, CCD camera, interface controller, and the computer system which controls and operates the system are shown schematically in Fig. 6. The control and operation of these systems are performed via the PDP 11-23 computer system; some of the computer programs which have been developed for this purpose are designated in Fig. 7.

Testing and operational verification of the new CCD camera have been performed since the new magnetograph was placed back at the observing site. Major emphasis has been placed on tests of sensitivity, linearity, S/N, lag, and fringing effects; results of these tests are described in the following paragraphs.

Sensitivity: The CCD camera as presently configured operates at a speed of 0.1s per exposure; this speed is determined by the camera read-out time rather than the exposure time. Tests performed on clear observing days when the Earth's atmosphere exhibits good transparency indicate that the CCD is sufficiently sensitive that saturation is achieved in exposure times shorter than 0.1s, with 0.06s exposures being typical. These results will allow us to redesign the CCD camera to operate at higher read-out speeds more compatible with the shorter exposure times. Currently the present system allows a complete vector magnetogram, enhanced 255 times, to be obtained in approximately 3.3m with a formal S/N of about 10^4. With the original system, a vector magnetogram similarly enhanced was obtained in 3.3m also, but with a S/N of only 10^3; to obtain a S/N of 10^4, approximately 10^4 enhancements would have been required with an increase in cycle time by a factor of about 40. Conversely, the new magnetograph can achieve the maximum S/N of the previous system (10^3) in approximately 1/30th the time ($\approx$7s).

Linearity: Results of tests for linearity of response for the CCD sensor are given in Fig. 8 which shows measured CCD signal versus camera exposure time for an unchanging, artificial light source. The measured signal is given as a percent of full scale, where full scale refers to the maximum number of counts that can be recorded with the 12 bits (4096) of the CCD's A/D converter.

S/N: Signal-to-noise analyses were performed using two identically-illuminated images together with a zero-signal image. The results given in Table II indicate that at a nominal illumination level of 80%, the expected S/N for a single, unenhanced intensity image will be $\approx$870; this is over an order of magnitude better than the measured S/N of the original system with the SEC vidicon, a value determined to be $\approx$70.

Lag: Measurements of signal retention by the CCD sensor show that approximately 0% of a previous image contributes to the read-out of a successive image.

Fringing: Fringe patterns can definitely be seen in intensity images obtained with the new camera system; these are interference patterns that result when a CCD is illuminated with monochromatic light. Thinned, glass-laminated CCD sensors exhibit at least two major interference effects in the thin (10 micron) silicon and in the glass. In a joint project between Kitt Peak National Observatory and Photometrics, Ltd., tests were made to measure the amplitude of fringing as a function of wavelength and to determine how efficiently a glass wedge inserted in the beam reduces the fringing. Results from these tests are summarized in Table III; they show that for wavelengths near that of the magnetograph's Zeiss filter (5250.22 Å), use of a wedge is essential, reducing as it does the peak-to-peak fringing modulation from 16% to 3%. We have acquired a glass wedge and plan to install it on the face of the CCD sensor as soon as tests are completed on techniques for removal of fringe patterns by photometric calibrations.

5. Performance of the New MSFC Magnetograph

Analyses of initial data obtained from observations of several sunspots and quiet solar areas show that the newly-upgraded magnetograph possesses far greater sensitivity than the previous system, detecting weak (1-2 G) fields in the line-of-sight component which were not previously observable. In Fig. 9, this increased sensitivity is explicitly evident in comparisons of line-of-sight magnetograms taken with different S/N levels (enhancements) for a complex sunspot group observed on August 2, 1983. The sunspots are shown in the "Intensity" frame at the lower right; indications of fringe patterns are visible in the lower right section of this intensity map. The two upper frames are the line-of-sight magnetic fields of these sunspots for two different S/N levels (theoretical): on the left, for "1024 enhancements," a S/N of $\approx 2 \times 10^4$; on the right, "256 enhancements," a S/N of $\approx 1 \times 10^4$. The line-of-sight field in the lower left frame represents the field as measured with the original MSFC magnetograph that had, at best, a S/N of 1×10^3. Comparisons of this latter frame with the upper ones indicate the enhanced sensitivity of the new system.

Versatility was another goal in this project. An aspect of this is shown in Fig. 10, which indicates the capability of nearly real-time data analysis and display on the Ramtek color-graphics terminal which is part of the data system. After obtaining raw observational data, displays such as this can be generated within minutes to show the line-of-sight magnetic field (upper left), transverse field (upper right), total field magnitude (middle left), angle of the field vector to the line-of-sight (middle right), and sunspot intensity (lower left). Such displays are useful, too, in comparing observations at different times, as in Fig. 11, which shows measurements of the vector magnetic field before and after a solar flare. The upper panels display the line-of-sight field component (left panel), the transverse component (middle), and sunspot intensities (right panel) as they were observed before the flare. The lower panels show the observed field and sunspots after the solar flare. The flare occurred near the sunspot which is in the center of the squares outlined on the line-of-sight fields. Such side-by-side displays, which could not be obtained with the old magnetograph system, are another facet of the versatility of the upgraded magnetograph.

The new data system now provides for enhanced capabilties in data analysis, allowing for the combination of color-graphic displays with contour drawings and line segments to depict field directions. In Figs. 12 and 13, data for the flare mentioned above have been manipulated to display the complete vector field: the line-of-sight component is represented by the colors (red and blue being positive and negative polarities, respectively), while the transverse component is represented in magnitude and direction by the length and orientation of the line segments. Figs. 12 and 13 represent the magnetic fields before and after the flare, respectively; the field-of-view of these figures corresponds to the outlined areas of Figure 11. Comparison of these kinds of data for solar flares can provide valuable documentation on changes in the vector field which occur during a flare.

Summary:

At the completion of this Discretionary Fund Program, we have developed a solar vector magnetograph with the capability of detecting 1-2 G fields in the line-of-sight component, approximately an order of magnitude better than the original system. Although final tests of the sensitivity in the transverse component are still in progress, we expect similar results there, also. As a result, the Marshall Center now has in operation a highly sensitive and versatile vector magnetograph for our continued research in solar-terrestrial physics and to support future NASA solar missions.

References

1. H. Zirin and K. Tanaka: Magnetic Transients in Flares, Astrophys.J., 250 (1981), p.791.

2. M.J. Hagyard, N.P. Cumings, E.A. West, and J.E. Smith: The MSFC Vector Magnetograph, Solar Phys.,80 (1982), p.33.

3. E.A. West: Extending the Field of View of KD*P Electrooptic Modulators, Appl. Opt.,17 (1978), p.3010.

Bibliography

"Computer Solutions for Studying Correlations between Solar Magnetic Fields and Skylab X-Ray Observations," D. Teuber, E. Tandberg-Hanssen, and M.J. Hagyard, Solar Phys.,53 (1977), p.97.

"The Spiral Configuration of Sunspot Magnetic Fields," M.J. Hagyard, E. West, and N.P. Cumings, Solar Phys.,53 (1977), p.3.

"Comparisons of Measured and Calculated Potential Magnetic Fields," M.J. Hagyard and D.L. Teuber, Solar Phys.,57 (1978), p.267.

"Extending the Field of View of KD*P Electrooptic Modulators," E.A. West, Applied Optics,17 (1979), p.3010.

"On the Presence of Electric Currents in the Solar Atmosphere," M.J. Hagyard, B.C. Low, and E. Tandberg-Hanssen, Solar Phys.,73 (1981), p.257.

"Analysis of the Vector Magnetic Fields of Complex Sunspots," S.R. Patty, in The Physics of Sunspots, Lawrence E. Cram and John H. Thomas, eds., Sacramento Peak Observatory, 1981.

"The Photospheric Vector Magnetic Field of a Sunspot and Its Vertical Gradient," M.J. Hagyard, E.A. West, E. Tandberg-Hanssen, J.E. Smith, W. Henze, Jr., et al., in The Physics of Sunspots, Lawrence E. Cram and John H. Thomas, eds., Sacramento Peak Observatory, 1981.

"Vector Magnetic Field Evolution and Associated Photospheric Velocity Shear within a Flare-Productive Active Region," K.R. Krall, J.B. Smith, Jr., M.J. Hagyard, E.A. West, and N.P. Cumings, Solar Phys.,79 (1982), p.59.

"The MSFC Vector Magnetograph," M.J. Hagyard, N.P. Cumings, E.A. West, and J.E. Smith, Solar Phys.,80 (1982), p.33.

"Observations of the Longitudinal Magnetic Field in the Transition Region and Photosphere of a Sunspot," W. Henze, Jr., E. Tandberg-Hanssen, M.J. Hagyard, E.A. West, et al., Solar Phys.,81 (1982), p.231.

"Active Region Magnetic Fields Inferred from Simultaneous VLA Microwave Maps, X-Ray Spectroheliograms, and Magnetograms," E.J. Schmahl, M.R. Kundu, K.T. Strong, R.D. Bentley, J.B. Smith, Jr., and K.R. Krall, Solar Phys., 80 (1982), p.233.

"Vertical Gradients of Sunspot Magnetic Fields," M.J. Hagyard, D. Teuber, E.A. West, E. Tandberg-Hanssen, W. Henze, Jr., et al., Solar Phys.,84 (1983), p.13.

"Interpretation of Vector Magnetograph Data Including Magneto-Optic Effects," E.A. West and M.J. Hagyard, Solar Phys.,88 (1983), p.51.

"Modelling of Energy Buildup for a Flare-Productive Region," S.T. Wu, Y.Q. Hu, K.R. Krall, M.J. Hagyard, and J.B. Smith, Jr., Solar Phys., in press (1984).

"Photospheric Electric Current and Transition Region Brightness Distributions," A.C. deLoach, M.J. Hagyard, D.M. Rabin, R.L. Moore, J.B. Smith, Jr., E.A. West, and E. Tandberg-Hanssen, Solar Phys., in press (1984).

"A Multiwavelength Study of a Double Impulsive Flare," K.T. Strong, J.B. Smith, Jr., et al., Solar Phys., in press (1984).

"A Quantitative Study Relating Observed Shear in Photospheric Magnetic Fields to Repeated Flaring," M.J. Hagyard, J.B. Smith, Jr., D. Teuber, and E.A. West, Solar Phys., in press (1984).

"Electric Currents in Active Regions," M.J. Hagyard, E.A. West, and J. B. Smith, Jr., in Proceedings of the International Workshop on Solar Physics and Interplanetary Travelling Phenomena, Chen Biao, ed., Kunming, People's Republic of China, 1984.

"The New MSFC Solar Vector Magnetograph," M.J. Hagyard, N.P. Cumings, and E.A. West, in Proceedings of the International Workshop on Solar Physics and Interplanetary Travelling Phenomena, Chen Biao, ed., Kunming, People's Republic of China, 1984.

"The Vertical Gradient of Sunspot Magnetic Fields," M.J. Hagyard, D. Teuber, E.A. West, E. Tandberg-Hanssen, and W. Henze, Jr., in Proceedings of the International Workshop on Solar Physics and Interplanetary Travelling Phenomena, Chen Biao, ed., Kunming, People's Republic of China, 1984.

TABLE I

Retardation Errors Over the Field-of-View

Retardation		Error in Retardation
Center Area	Left Corner	
89.576^{o}	86.916^{o}	2.66^{o}
90.132^{o}	87.478^{o}	2.65^{o}
88.848^{o}	91.530^{o}	-2.68^{o}
93.629^{o}	89.845^{o}	3.78^{o}

Table II

S/N Tests With Solar Source

Illumination Level (% of Saturation)	S/N*
92	918
82	869
79	869
74	845
68	756
63	759
60	764
52	706
43	649
42	642

*Defined as number of A/D counts (S) divided by $\sqrt{S}$.

Table III

Measurements of Fringing in a Thinned Glass-Laminated CCD

Wavelength	Peak-to-Peak Fringing Modulation	
	No Wedge	With Wedge
4500Å	3%	2%
5600Å	16%	3%
7500Å	30%	12%

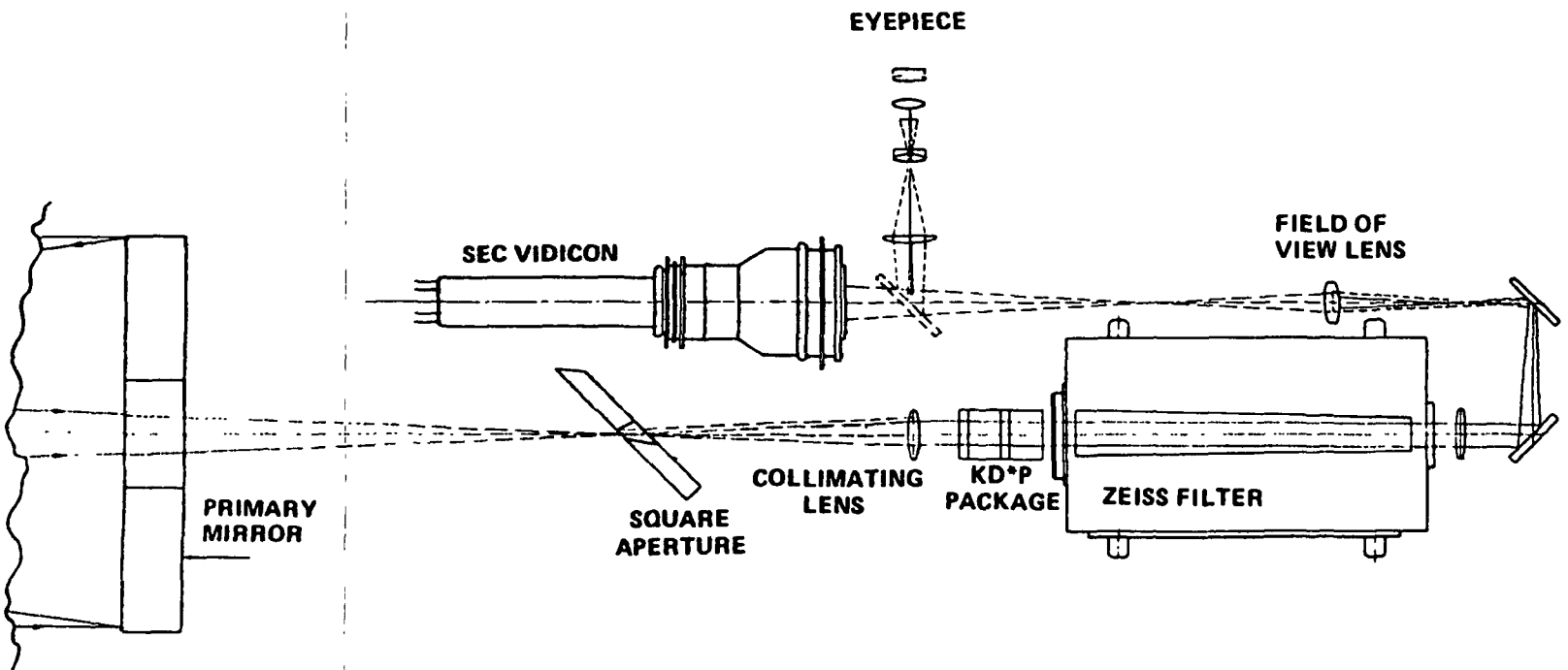

Figure 1: Schematic diagram of the optical system of the original MSFC vector magnetograph.

Figure 2

NEW POLARIMETER FOR MSFC VECTOR MAGNETOGRAPH

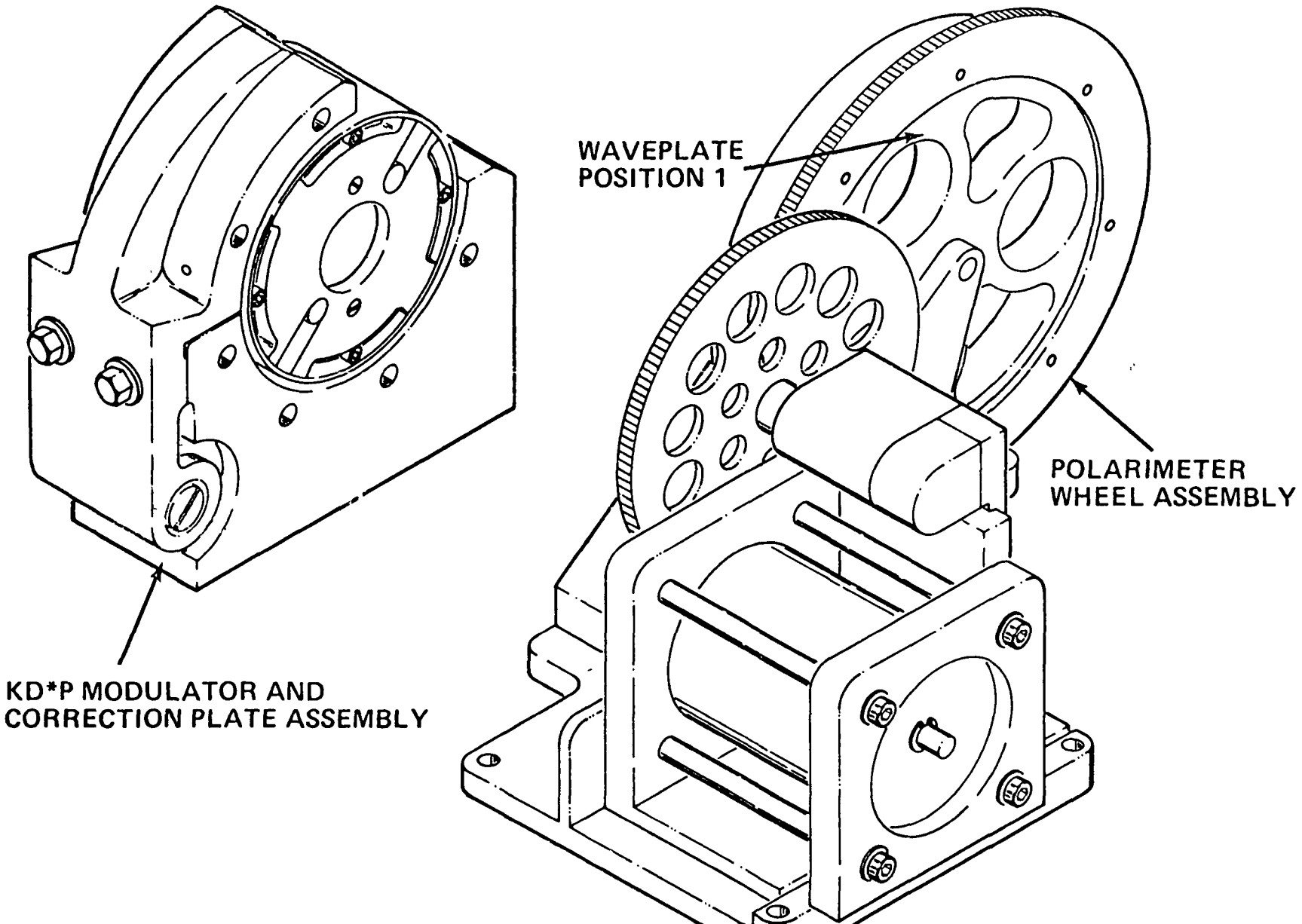

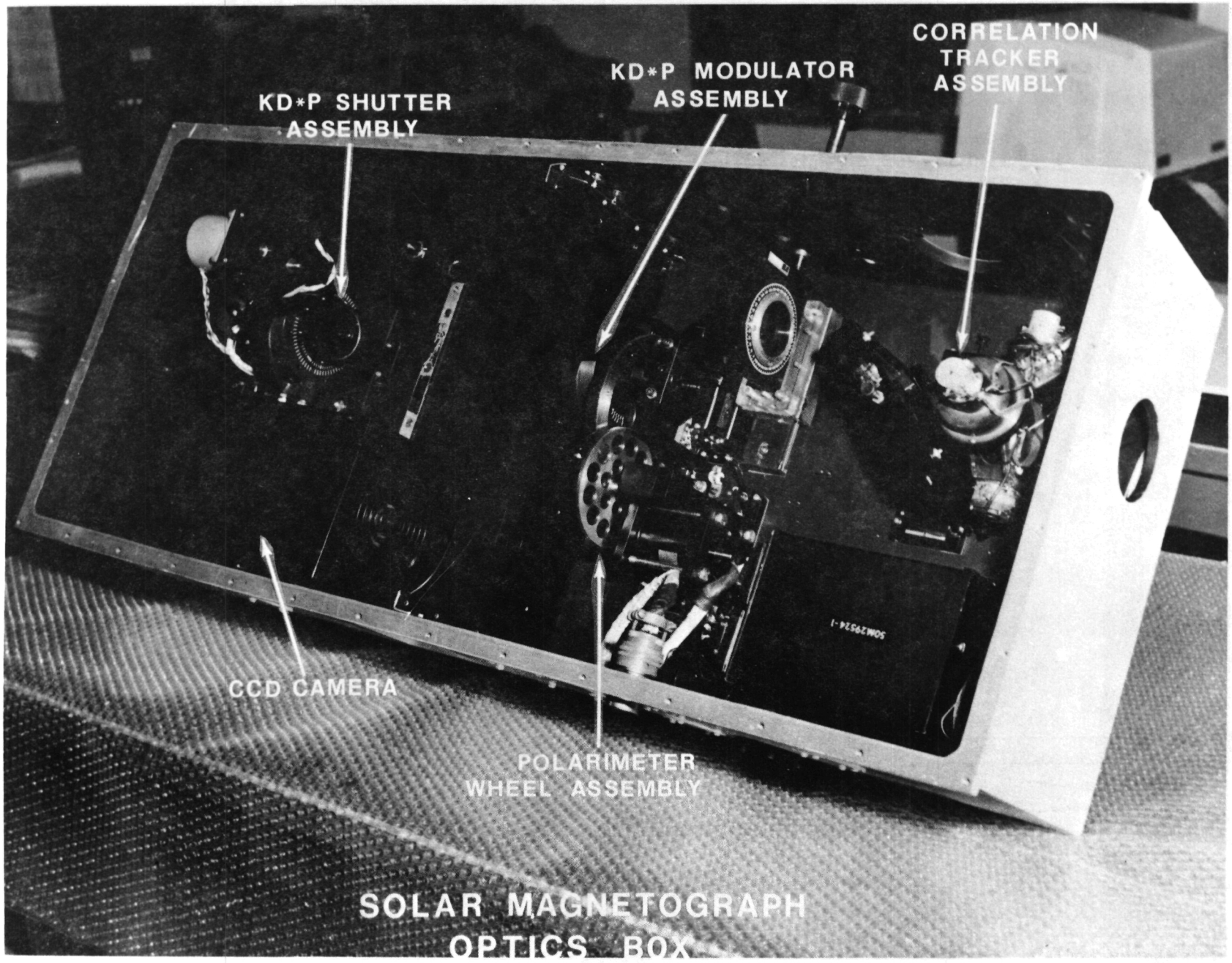

Figure 3: Photograph of the new optics box (without the Zeiss filter).

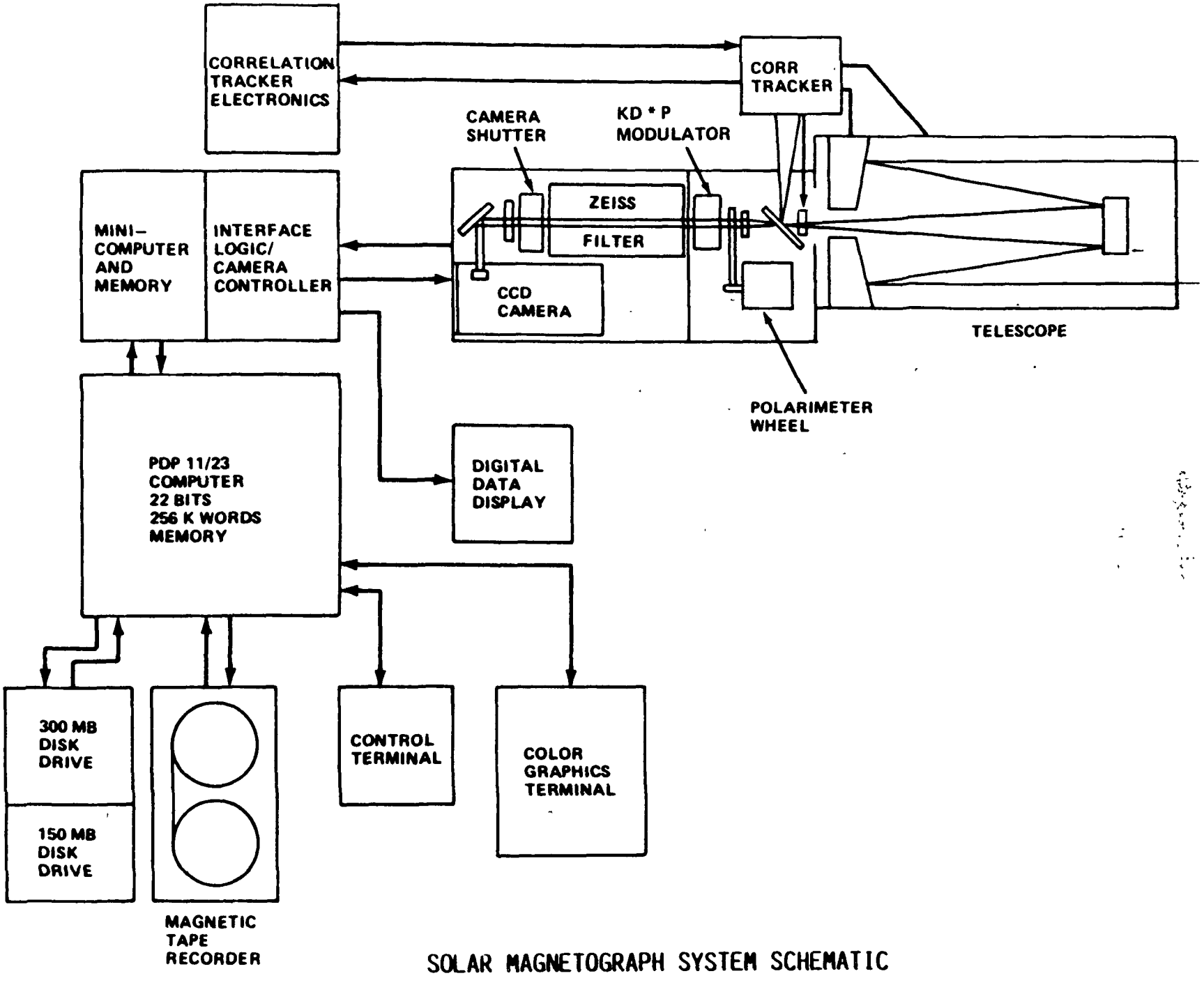

Figure 4: Schematic depiction of the new system. Light from the telescope enters the optics box containing the new polarimeter and CCD camera.

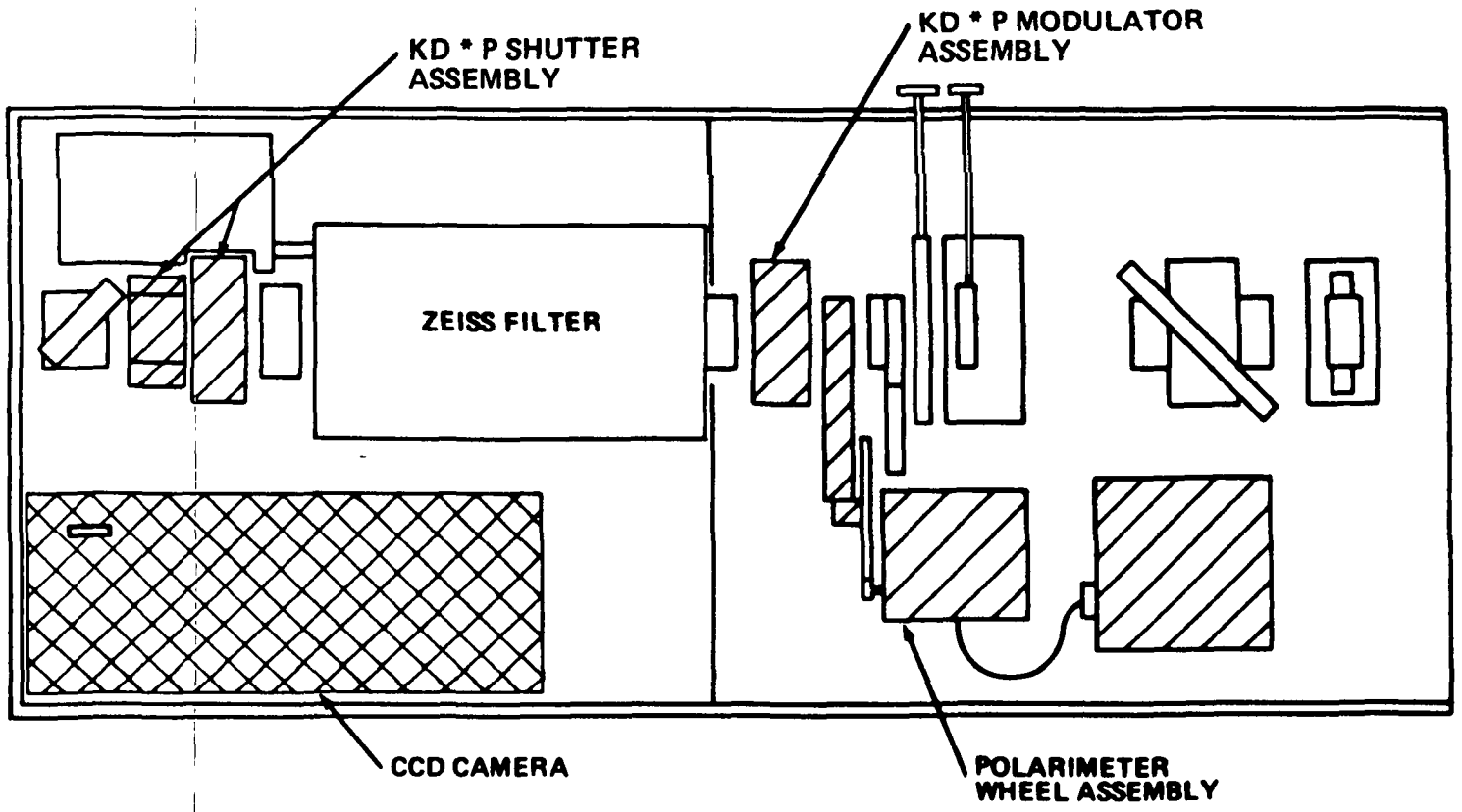

Figure 5: Schematic configuration of the new optics box.

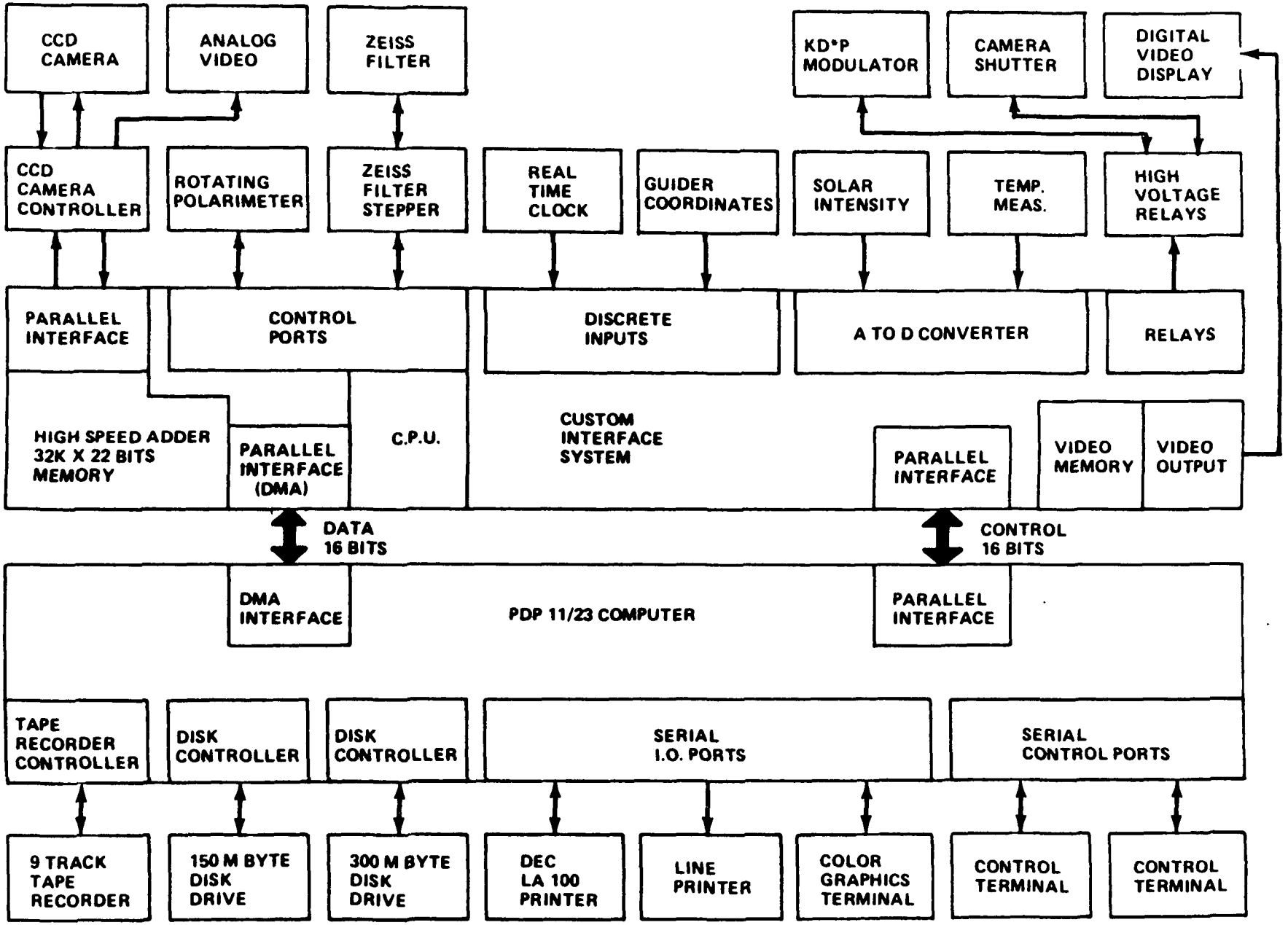

SOLAR MAGNETOGRAPH CONTROL SYSTEM

Figure 6: Diagram of the complex interfaces between the new control system and the magnetograph.

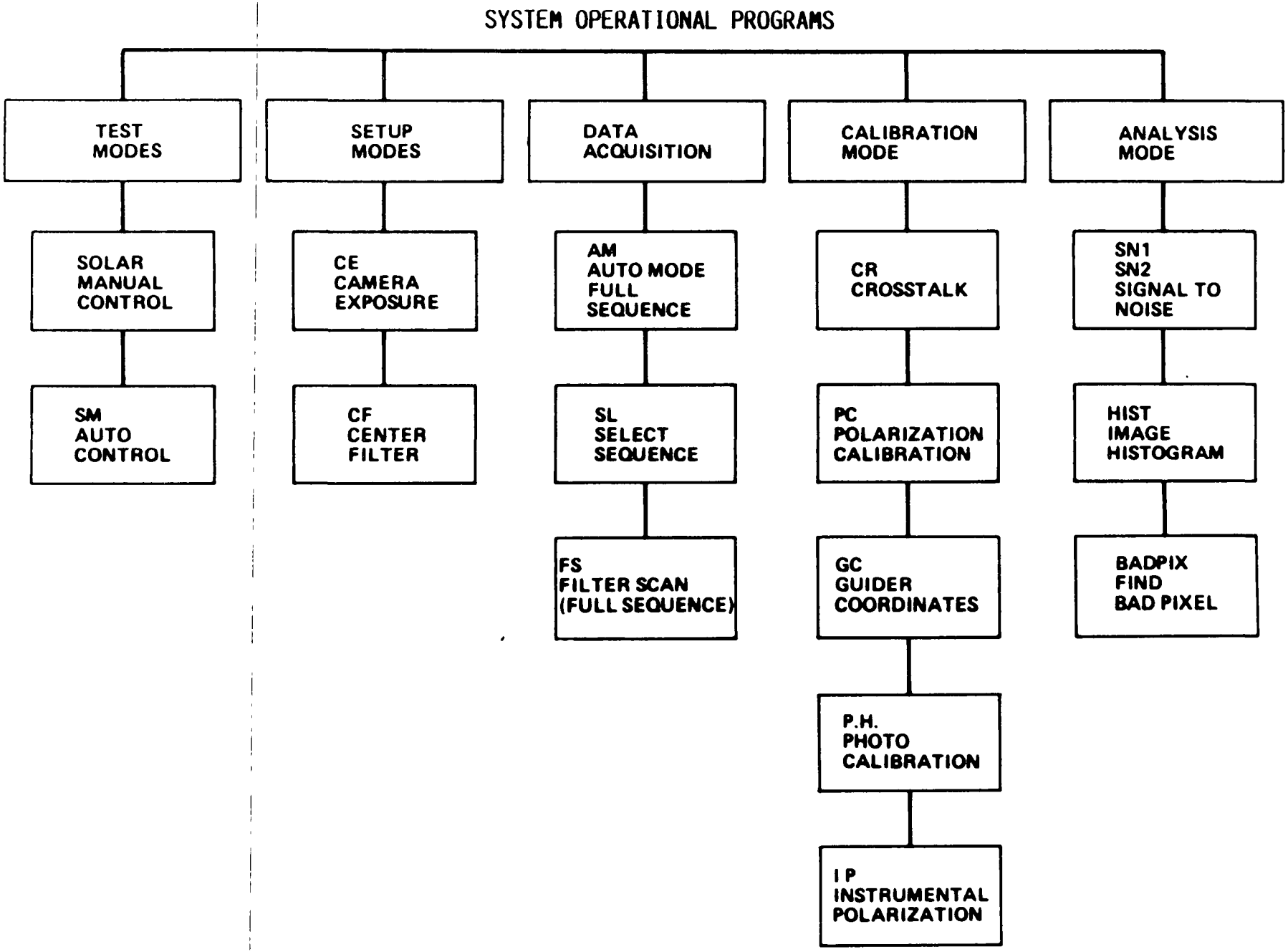

Figure 7: Computer programs developed for control and operation of the new magnetograph.

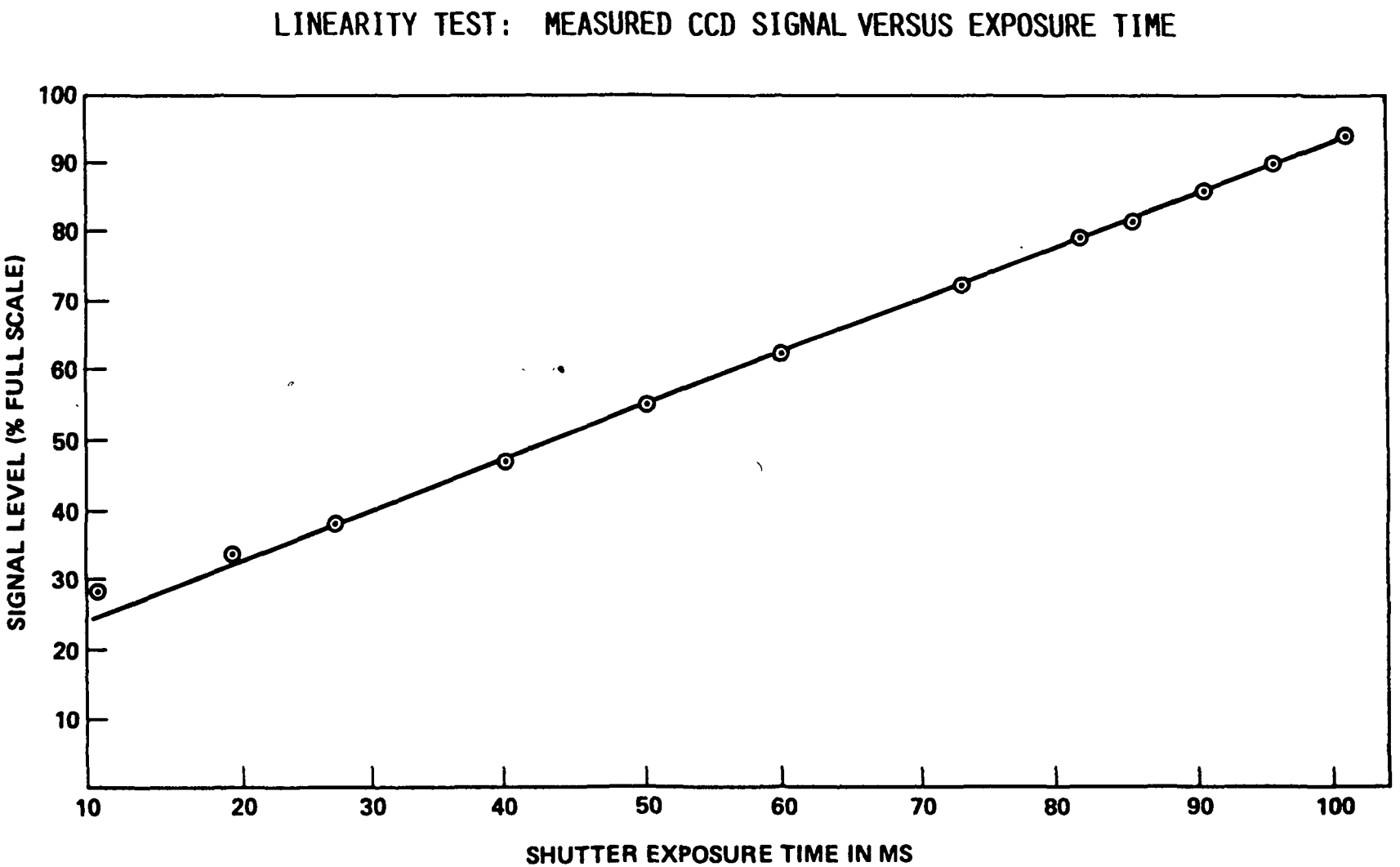

Figure 8: Results of linearity tests. The measured signal level, expressed as a percent of full-scale signal, is shown to be a linear function of illumination incident on the CCD detector as measured by the exposure time of the detector.

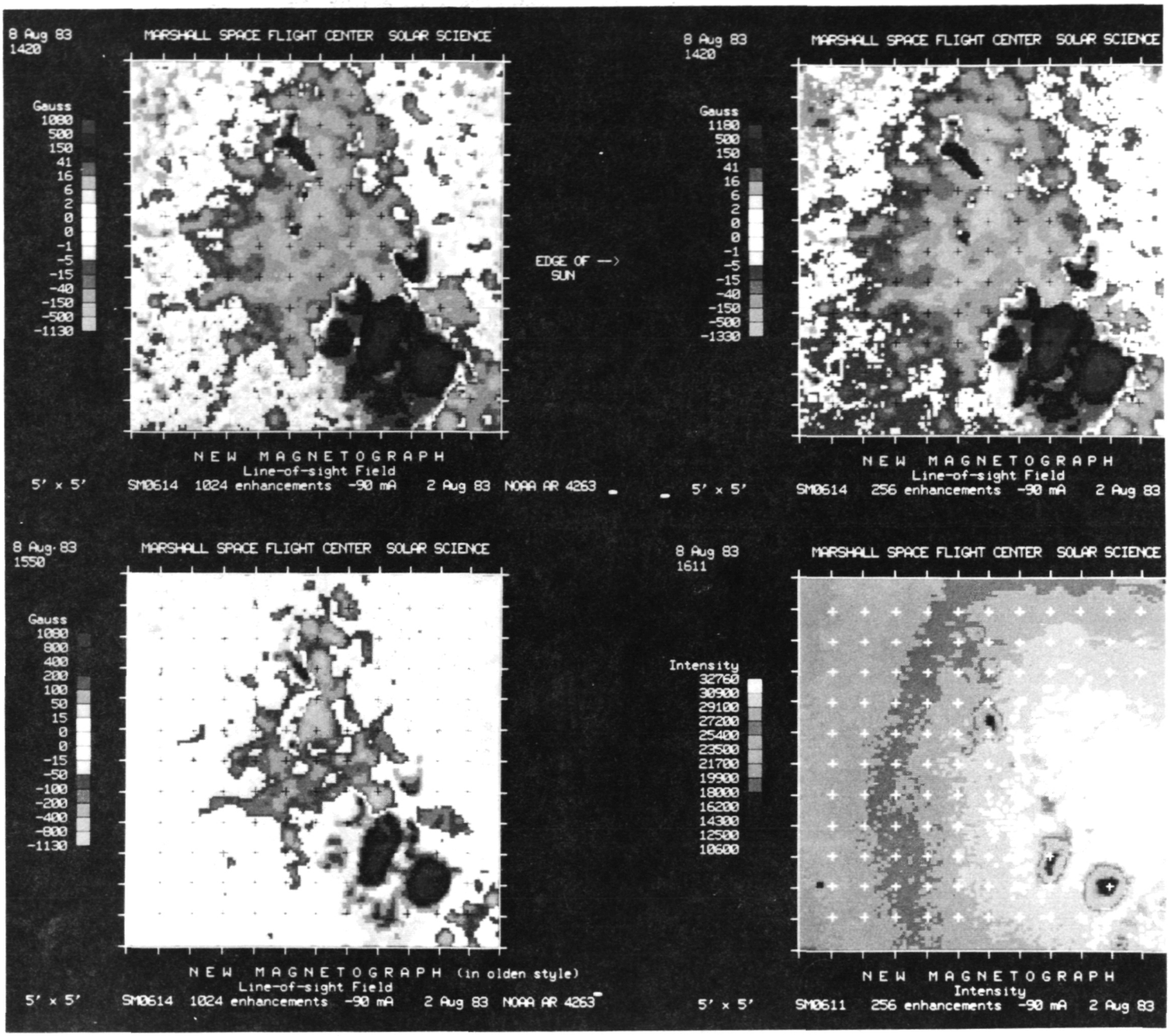

Figure 9: Initial magnetic field data indicating the sensitivity of the new magnetograph. The two upper frames portray the line-of-sight magnetic fields of the sunspot group shown in the lower right frame; fields of 2 gauss are discernible. The lower left frame shows this line-of-sight field as measured with the original system; the sensitivity is about 15 gauss.

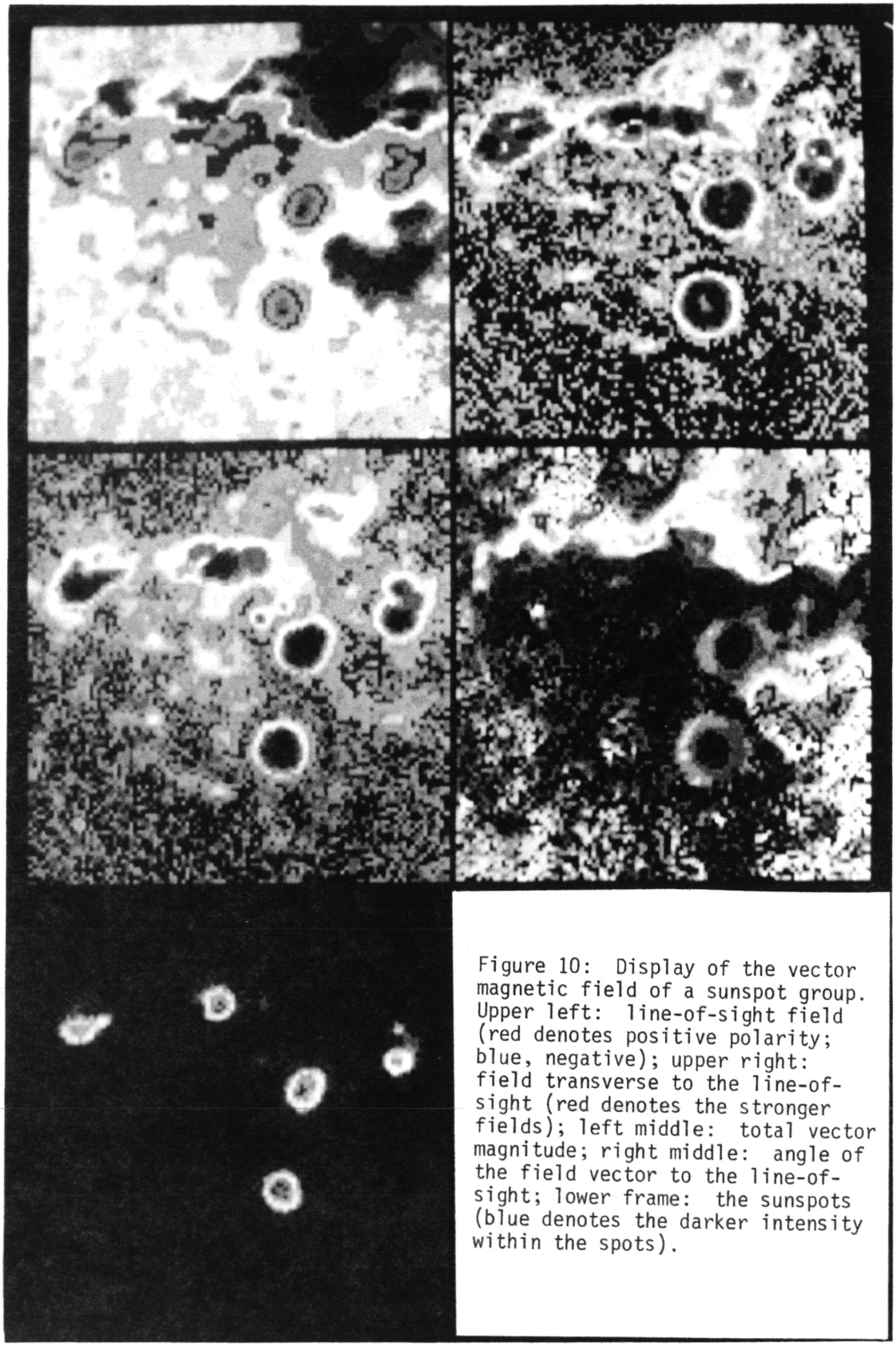

Figure 10: Display of the vector magnetic field of a sunspot group. Upper left: line-of-sight field (red denotes positive polarity; blue, negative); upper right: field transverse to the line-of-sight (red denotes the stronger fields); left middle: total vector magnitude; right middle: angle of the field vector to the line-of-sight; lower frame: the sunspots (blue denotes the darker intensity within the spots).

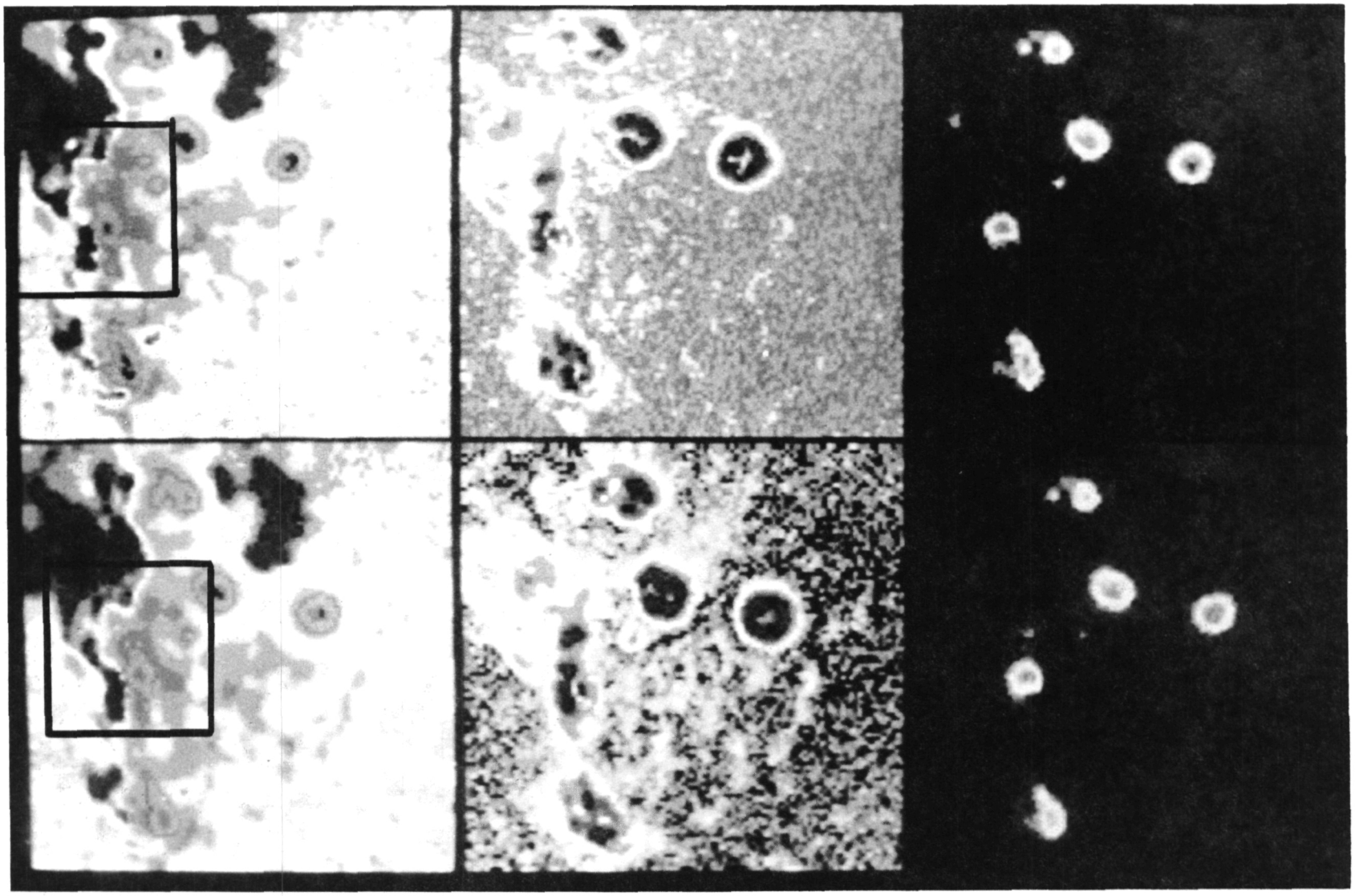

Figure 11: Vector field of a sunspot group before and after a solar flare. The top panels, left to right, represent the line-of-sight field, transverse field and sunspot intensities observed prior to a solar flare. The lower panels show the same field components observed after the flare occurred near the sunspot to the left of center. The outlined squares indicate enlarged areas shown in Figures 12 and 13. The field-of-view of each panel is 5.7x5.7 arc minutes.

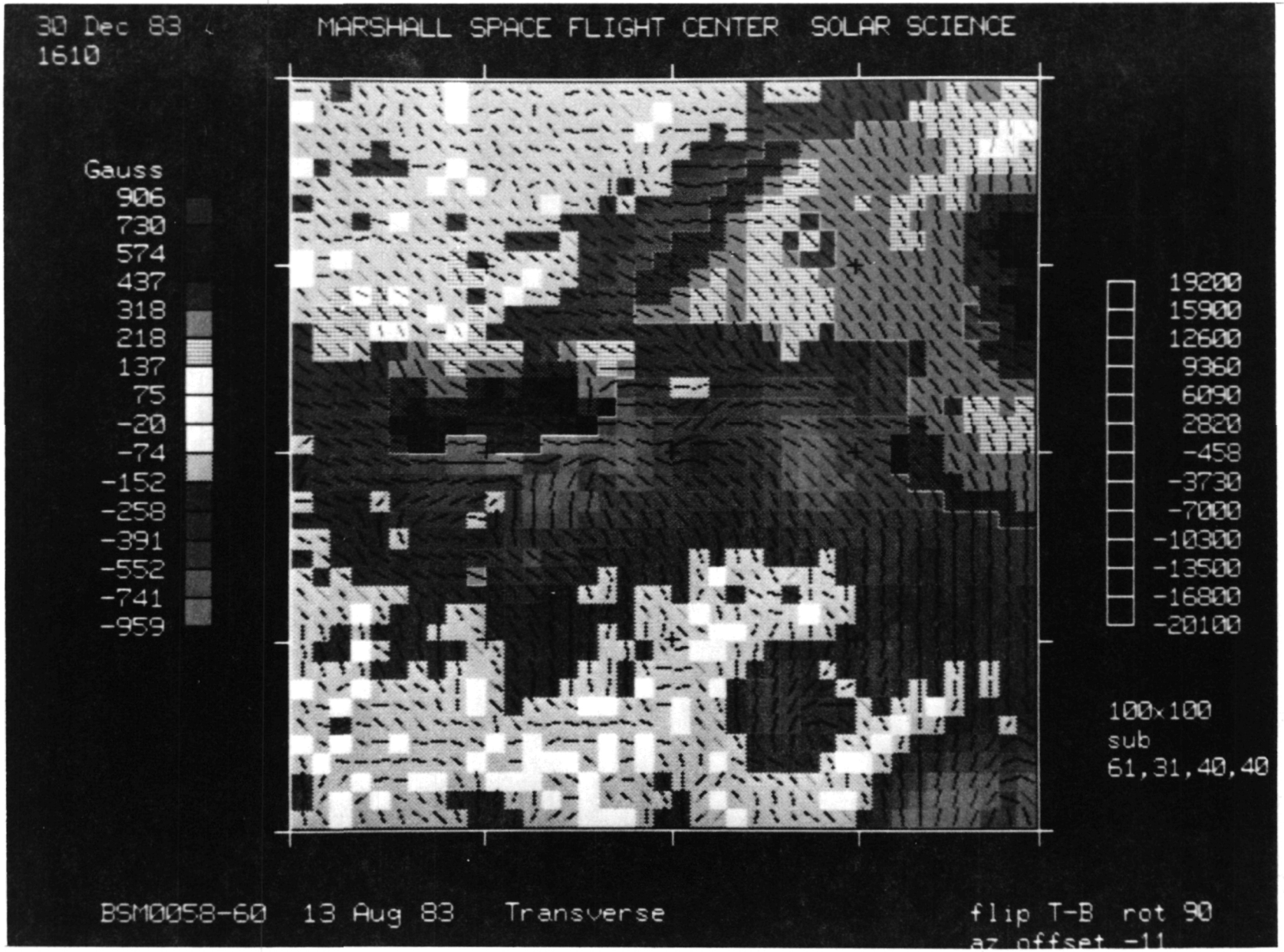

Figure 12: Vector magnetic field before the flare of August 13, 1983. The field-of-view displayed is the area outlined in Figure 11, centered on the flaring region.

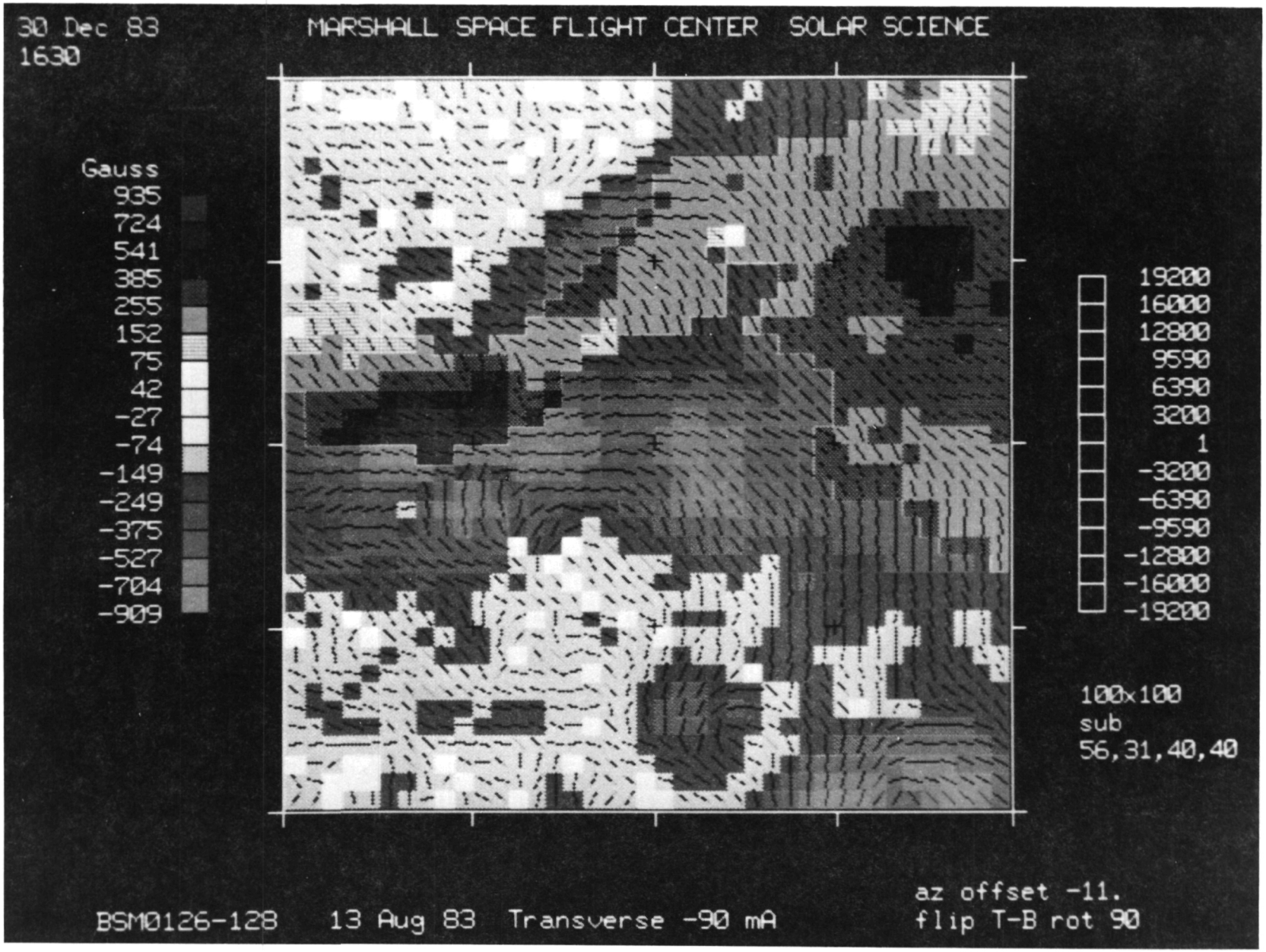

Figure 13: Vector magnetic field after the flare of August 13, 1983. The field-of-view again corresponds to the outlined area in Figure 11 where the flare occurred.

APPROVAL

THE NEW MSFC SOLAR VECTOR MAGNETOGRAPH

By M. J. Hagyard, E. A. West, and N. P. Cumings

The information in this report has been reviewed for technical content. Review of any information concerning Department of Defense or nuclear energy activities or programs has been made by the MSFC Security Classification Officer. This report, in its entirety, has been determined to be unclassified.

E. Sandberg-Hanssen

Alexander J. Dessler
Director
Space Science Laboratory